Quantum Memory Testbed Based on Nitrogen-Vacancy Centers in Diamond

Julie Chen [1], Tommy Nguyen [2], Victor Marcenac [1], Weitao He [2], Kai-Mei C. Fu [1 2 3], Maxwell F. Parsons [1]

[1]Department of Electrical & Computer Engineering, University of Washington [2]Department of Physics, University of Washington, University of Washington [4]Pacific Northwest National Laboratory

Motivation

Negatively charged nitrogen-vacancy (**NV⁻**) centers in diamond are ideal for studying quantum control, open quantum systems, and multi-qubit entanglement:

- NV⁻ centers have long spin coherence times and accessible optical transitions at 4 Kelvin.
- A single NV⁻ center is naturally coupled to nearby nuclear spins via dipolar interaction, which allows for a system with more than 10 fully characterized qubits.
- Optical access for spin initialization and readout, and MW/RF for quantum gates.

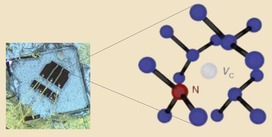

Left: Diamond surface with a fabricated antenna.
Right: Atomic structure of the NV center, consisting of a substitutional nitrogen and adjacent vacancy.

Cryogenic Confocal Microscope

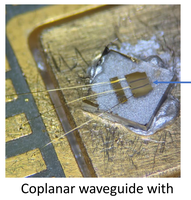

Coplanar waveguide with wire-bond fabricated on diamond surface

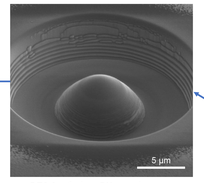

SEM of the SIL; enhances photon collection efficiency by ~10x

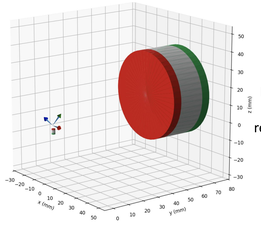

Internal and External Magnet position relative to the NV's axis

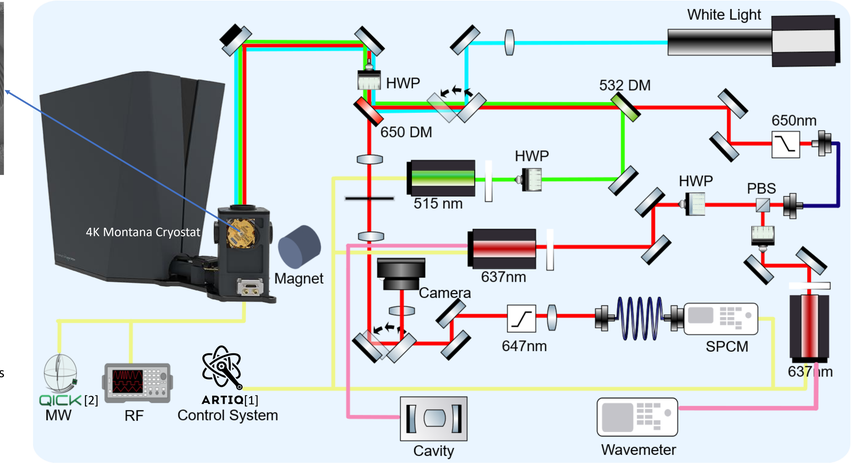

Resonant control

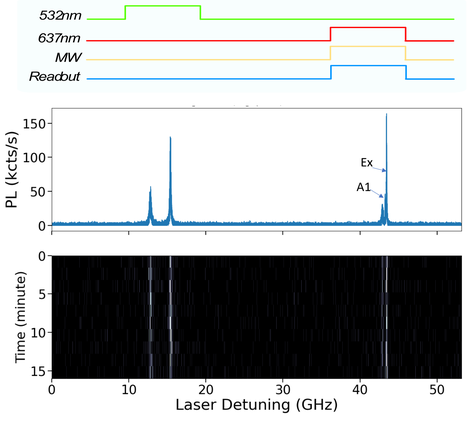

Photoluminescence Excitation spectra of the NV center. Blue arrow indicates the transitions Ex(A1) to optically pump the NV into ms = −1(ms = 0).

NV energy level structure

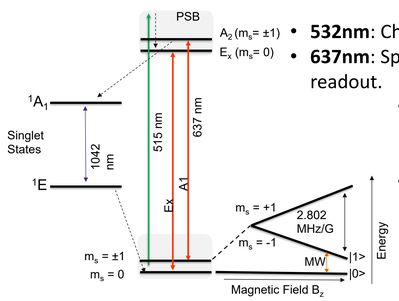

- **532nm**: Charge initialization into m_s= 0.
- **637nm**: Spin initialization and optical readout.
- **Magnetic field B_z**: induces Zeeman splitting of the m_s=±1 levels.
- **Resonant MW**: drive transitions between m_s=0 and m_s=±1.

MW/RF control

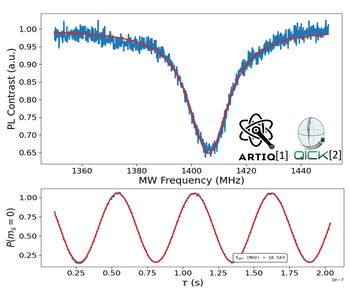

- Rabi Oscillations and Optically Detected Magnetic Resonance with a magnetic field B_z=525G.
- MW and laser control using hybrid FPGA system composed of QICK and ARTIQ at 200ps resolution.
- MW Pulse error characterization to achieve accurate $\pi_{x,y}$ and $\pi/2_{x,y}$ pulses [3].
- Achieved 99% and 97% accuracy for π_x and π_y pulses.

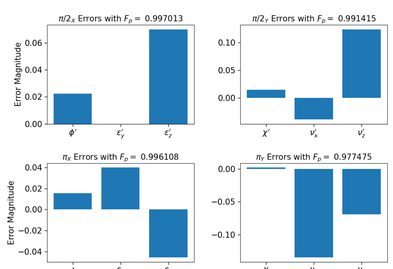

Current Results

- Single shot readout with average m_s=0 and m_s=-1 fidelity of 87.15%.
- Dynamical Decoupling enhances NV electron spin coherence, while the characteristic dips occur at a nuclear spin resonance where the electron gets entangled with a nearby ^{13}C spin.
- The orange curve represents a fit to the data, identifying 9 unique nuclear with their associative hyperfine coupling strengths.
- Scanning the radio frequency during the DDS enhances nuclear spin detection by resolving weakly coupled ^{13}C nuclei.

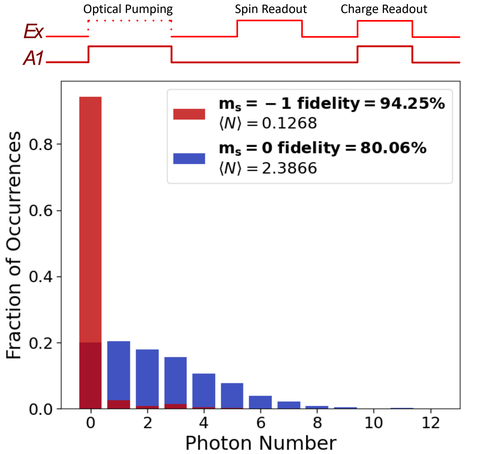

Projective single-shot readout of the NV⁻ electronic spin

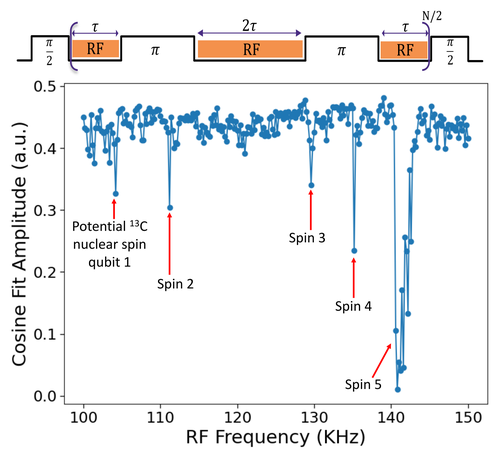

Dynamical Decoupled Radio Frequency (DDRF)

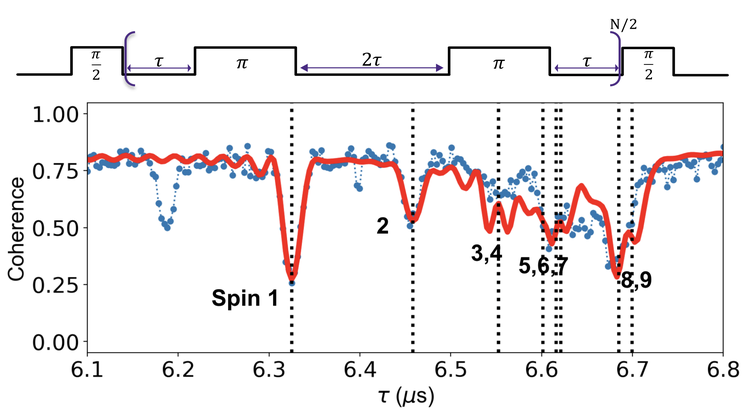

Dynamical Decoupling Spectroscopy (DDS)

Spin	$\omega_h/2\pi$ (kHz)	θ (deg)
1	133.059	68.610
2	50.282	44.927
3	51.398	69.341
4	51.356	69.319
5	31.748	101.337
6	44.654	95.552
7	92.178	90.898
8	80.027	88.124
9	69.168	85.927

Identified spins with their respective hyperfine coupling strength and orientation angle

Next Steps

- Machine Learning assisted nuclear spin spectroscopy.
- Nuclear spin polarization enhancement.
- Quantum error correction for correlated dephasing [4].
- Multi-qubit entanglement with parallel scheme [5].

Acknowledgements and References

This work was supported by NIST 60NANB23D202, NSF PHY-GRS 2233120, DMR-2019444, and Sandia National Laboratories.

[1] QICK. *QICK documentation*. docs.qick.dev (2024).
[2] M-Labs. *ARTIQ manual*. m-labs.hk/artiq (2026).
[3] Dobrovitski, V. V. *et al. Phys. Rev. Lett.* **105**, 077601 (2010).
[4] Layden, D. *et al. Phys. Rev. Lett.* **124**, 020504 (2020).
[5] Takou, E. *et al. Phys. Rev. X.* **13**, 011004 (2023).